

Errors introduced in a-Si:H-based solar cell modeling when dangling bonds are approximated by decoupled states

E. Klimovsky^a, J.K. Rath^b, R.E.I. Schropp^b, F.A. Rubinelli^{a,*}

^aINTEC, Universidad Nacional del Litoral, Güemes 3450, 3000 Santa Fe, Argentina

^bUtrecht University, Debye Institute, P.O. Box 80000, 3508 TA Utrecht, The Netherlands

Received 10 December 2001; received in revised form 5 September 2002; accepted 20 September 2002

Abstract

In this paper we investigate in a-Si:H-based devices the accuracy of approximating dangling bonds by pairs of donor-like and acceptor-like states. We discuss the impact of using this approximation in device modeling by studying the dark current–voltage, the illuminated current–voltage and the spectral response curves. We find that the relative error introduced by this approximation in these characteristic curves can be tolerated when the correlation energy is assumed to be positive and when the capture cross-section of neutral states adopted is much smaller than that of charged states. A wide range of intrinsic layer-thickness values, density of states and temperatures has been investigated. This approximation fails when the correlation energy adopted is negative, and is not accurate enough when the correlation energy is assumed to be positive but the capture cross-section of neutral states adopted is higher than that of charged states.

© 2002 Elsevier Science B.V. All rights reserved.

Keywords: Amorphous materials; Solar cells; Donor and acceptor states; Amphoteric states

1. Introduction

Hydrogenated amorphous silicon-based semiconductors (a-Si:H, a-SiGe:H, a-SiC:H) contain a large number of localized states in the mobility gap. These states strongly influence their electrical and optical properties, acting simultaneously as trapping and recombination centers. States in the conduction and valence bands are single-electron states that behave as acceptor and as donor states, respectively. On the other hand, there is considerable evidence supporting the fact that deep states arising from dangling bonds (DBs) have an amphoteric character, behaving simultaneously as donors and acceptors [1]. Okamoto et al. derived in 1984 analytical expressions for the occupation function and for the recombination rate of amphoteric states [2]. However, it is still common practice, at least in steady-state processes, to represent a-Si:H DB by pairs of decoupled (donor-like and acceptor-like) and independ-

ent electron states [3–5]. As the occupation functions and recombination rates of amphoteric states are different from their counterparts in single-occupied states, this approximation could lead to some degree of inaccuracy.

The errors introduced by modeling DB with decoupled states have been already discussed in the literature, but the inexactness of this approximation has only been explored for materials in which the electrical properties are uniform. In this paper we discuss the errors introduced by the decoupled states on the output characteristics of solar cells. We compare, in a-Si:H-based devices, the current–voltage (J – V) and the spectral response (SR) curves when DBs are represented with decoupled states or with amphoteric states. In this study we use realistic electric and optical input parameters resulting from fitting experimental solar-cell J – V and SR characteristics. Our paper is organized as follows: in Section 2 we summarize the two approaches and the results already available in the literature; in Section 3 we show our fittings of a-Si:H p–i–n solar-cell characteristics; in Section 4 we discuss how accurate the approximation of decoupled states is in reproducing J –

*Corresponding author. Tel.: +54-342-455-9174; fax: +54-342-455-0944.

E-mail address: pancho@intec.unl.edu.ar (F.A. Rubinelli).

V and SR characteristics; and finally in Section 5 we discuss this approximation in other materials and scenarios.

2. Short description of the two approaches and review of previous results found in the literature

2.1. Formalism

Let us first assume that we have a density N_T (cm^{-3}) of donor-like localized states at energy E_1 and of acceptor-like states at energy E_2 . The following basic processes compete in order to define the occupation functions and the recombination rate at E_1 and at E_2 :

Electron emission: (T₁) $E_1^0 \rightarrow E_1^+ + e$; (T₅) $E_2^- \rightarrow E_2^0 + e$

Electron capture: (T₂) $E_1^+ + e \rightarrow E_1^0$; (T₆) $E_2^0 + e \rightarrow E_2^-$

Hole emission: (T₃) $E_1^+ \rightarrow E_1^0 + h$; (T₇) $E_2^- \rightarrow E_2^- + h$

Hole capture: (T₄) $E_1^0 + h \rightarrow E_1^+$; (T₈) $E_2^- + h \rightarrow E_2^0$

The nomenclature is as follows: +, 0 and – stand for positive, neutral and negative charge of the dangling bond, e for an electron and h for a hole. Let us now assume that we have a density N_T (cm^{-3}) of amphoteric states at energy E_1 with correlation energy U , where U is defined as $U = E_2 - E_1$; E_1 is the energy of the first electron and E_2 is the energy of the second electron. In the first scenario, N_T dangling bonds are represented by the decoupled approach and in the second, N_T dangling bonds are represented by amphoteric states. The same eight processes describe the kinetics and define the occupation functions and the recombination rate in both cases, but in the first scenario the processes T₅–T₈ are independent of processes T₁–T₄, and in the second scenario they are correlated. In the decoupled approach the electron occupation function and the recombination rate are given by the well-known expressions derived by Shockley–Read–Hall [3]. These expressions are applied to both donor-like and acceptor-like states. Donor-like states are positively charged when they are empty and acceptor-like states are negatively charged when they are occupied; otherwise they are neutral. They can host no more than one electron. If we want to indicate explicitly the state charge status before the capture of a free carrier, we could use the following notation for the cross sections: σ_n^+ for electron capture cross-section at energy E_1 ; σ_n^0 for electron capture cross-section at energy E_2 ; σ_p^- for hole capture cross-section at energy E_2 ; and σ_p^0 for hole capture cross-section at energy E_1 . Below we refer to charged cross-sections σ_{CH} meaning σ_n^+ or σ_p^- and to neutral cross-sections σ_0 meaning σ_n^0 or σ_p^0 . When states are assumed to be amphoteric, the occupation functions and recombination rate are given by expressions derived by Okamoto et al. [2]. The cross-section symbols have similar meanings,

but the energy levels E_1 and E_2 are usually noted by $E^{+/-}$ and by $E^{0/-}$, respectively.

In a-Si:H-based materials, we have a continuous density of dangling bonds ' $N_T(E)$ ' and we should perform the integration over the energy values E of the whole mobility gap to obtain the total trapped charge density and the total recombination rate.

2.2. Review of previous results

Assuming that the correlation energy U is positive and much larger than the thermal energy kT , Halpern [6] claimed that for steady-state processes, dangling bonds behave, to an excellent approximation, like a pair of independent electron states. Under thermodynamic equilibrium, he showed that the net charge is identical in an amphoteric state having energy E_1 and E_2 , and in a donor- and acceptor-state pair, energy E_1' and E_2' , defined as $E_1' = E_1 - kT \ln 2$ and $E_2' = E_2 + kT \ln 2$. Under no equilibrium he concluded that assuming that: (a) $U \gg kT$, (b) the capture cross sections for charged centers (σ_{CH}) are appreciably larger than that for neutral centers (σ_0), and (c) the ratio σ_n^+/σ_n^0 is close to the ratio σ_p^-/σ_p^0 , then the decoupled approach is a good approximation. He did not include any specific calculation comparing the two net charges and recombination rates. Finally, using the demarcation level concept [7], he also showed that the decoupled approach always provides accurate values for the net charge per dangling bond, but sometimes leads to an appreciable error in the recombination rate. He claimed that the decoupled approach overestimates the fraction of unoccupied dangling bonds in n-type materials and the fraction of occupied dangling bonds in p-type materials.

Suntharalingam and Branz [8] also concluded that the decoupled approach is accurate when the correlation energy U is positive and $U \gg kT$. Making some intuitive assumptions, they discussed the physics of amphoteric states relying only on expressions belonging to the decoupled approach. They added to the results of Halpern that the errors introduced in the recombination rate are less than or equal to $\sigma_0/\sigma_{\text{CH}}$. Finally, they noted that the density of neutral states is overestimated by the decoupled approach.

Willemsen [9], in Appendix B of his PhD thesis, presented a numerical analysis performed on p-, i- and n-type materials. Not making any a priori assumption or approximation, he calculated Δf and $\Delta \eta$, where Δf is the absolute error in the occupation function and $\Delta \eta$ is the relative error in the recombination rate introduced by the decoupled approach. His main results are that the error Δf is only significant in intrinsic materials and that the error $\Delta \eta$ equals $\sigma_{\text{CH}}/\sigma_0$ for minority carriers. He also concluded that the amphoteric model can be approximated by a pair of donor-like and acceptor-like

states if $\sigma_0 \ll \sigma_{CH}$ and if $U > 0$ and is considerably larger than the thermal energy kT .

These authors discussed the decoupled approach only in materials and they treated separately the errors introduced by this approximation in the occupation functions and in the recombination rate. This is not really the case in solar cell modeling, where the Poisson and continuity equations are simultaneously solved. An error introduced by the recombination rate could affect the resultant gap-state occupation functions. Recombination rates and occupation functions cannot be treated as independent entities in device modeling. Hence, it is interesting to explore the errors introduced by the decoupled approach when it is used in the evaluation of device characteristic curves.

3. Fitting of a-Si:H solar-cell experimental curves

Single p–i–n a-Si:H solar cells were grown by plasma-enhanced chemical vapor deposition (PECVD) in an ultra-high-vacuum multi-chamber system (PASTA). Cells were deposited on SnO₂-coated glass (Asahi U-type) in the super-substrate configuration SnO₂/p-a-SiC:H/i-a-Si:H/n-a-Si:H/Ag. Three very thin layers with decreasing content carbon were included between the p- and the intrinsic layers. The intrinsic layer is 500 nm thick and the p–i–n structure is in the annealed state. The absorption coefficient and refractive index of each individual a-Si:H layer were determined by $R-T$ measurements. The total density of dangling bond and the Urbach tail were extracted with the CPM technique. The activation energy of each single layer was obtained from the temperature dependence of the dark conductivity. Single a-Si:H p–i–n solar cells were characterized by measuring the AM1.5 light $J-V$ response, the spectral response (SR) and the dark $J-V$ characteristics.

Our simulations were performed with the computer code D-AMPS (Analysis of Microelectronic and Photonic Devices) [10] developed at Pennsylvania State University, USA, plus some new developments. In this paper we simultaneously model the density of dangling bonds using uniform densities of gap states in each device layer (UDM) and the defect pool model (DPM) as proposed by Powel and Deane [11,12]. The density of states in the UDM model is described with three different Gaussian distributions, recognized as D^- , D^0 and D^+ . The peak energy of these Gaussian functions are located in the lower half of the bandgap (D^-), close to the Fermi level of the intrinsic material (D^0), and in the upper half of the bandgap (D^+). The ratio of charged to neutral defects adopted is 4:1. The Gaussian peaks are spaced by 0.3 eV in energy along the whole device, and consequently the separation between the non-occupied D^+ peak and the double-occupied D^- peak, usually known as Δ , is adopted equal to 0.4 eV, independent of the bandgap. In the DPM approach, the

total hydrogen concentration H is assumed to be $5 \times 10^{21} \text{ cm}^{-3}$, the correlation energy is fixed at 0.2 eV and the adopted freezing temperature adopted is 500 K. The most probable energy E_p in the distribution of available states is used as a ‘pseudo-free’ fitting input parameter and the pool width is appropriately selected to reproduce the same value of $\Delta = 0.4 \text{ eV}$ in each layer. Among the three different microscopic chemical reactions proposed by Powel and Deane, we selected the reaction where only one Si–H bond is broken [11]. The other two alternative mechanisms give rise to either too low or too high a density of DBs.

The activation energy in both doped layers was derived from dark conductivity measurements. Their values in the p- and n-type layers were 0.47 and 0.24 eV, respectively. The input electrical parameters not directly measured were adopted from the literature or from our best fittings. For instance, the electron and hole mobilities are 20 and $2 \text{ cm}^2 \text{ V}^{-1} \text{ s}^{-1}$ in a-Si:H, respectively, and two-fold lower in a-SiC:H. The effective density of states N_c and N_v are assumed to be $2 \times 10^{20} \text{ cm}^{-3}$, and the capture cross-sections adopted are 5×10^{-15} and $5 \times 10^{-16} \text{ cm}^2$ for charged and neutral gap-states, respectively, in both tails and mid-gap states. Since there is not yet a clear picture available for the distribution of energy offsets, we split the bandgap offsets equally between the conduction and the valence band at each interface. The total density of DBs and the valence-band tail slope were determined from CPM experiments as $5 \times 10^{15} \text{ cm}^{-3}$ and 48 meV, respectively. The conduction-band tail slope is assumed to be 30 meV. In order to account properly for the scattering of light on textured substrates, a pseudo Monte Carlo method was implemented. In our optical model, the main light beam is divided into several sub-beams of lower intensity, but keeping the total intensity unaltered. The reflection and refraction of each sub-beam at rough surfaces were modeled by introducing a random angle allowed to vary between a maximum and a minimum. The difference between the maximum and the minimum angle accounts for the roughness of each interface.

Fig. 1 shows the experimental dark and illuminated current–voltage ($J-V$) curves and our best fits. We can observe in this figure that it is possible to fit $J-V$ curves and the spectral response SR (not shown in this paper) using either the UDM or the DPM approach. Except for the DB density, all the electrical and optical parameters were assumed to be identical in both representations. Table 1 gives the total DB density and the most probable energy E_p in the UDM and DPM models, respectively, used to fit the $J-V$ and SR experimental curves. Fittings were performed assuming that DBs have an amphoteric nature in every device layer.

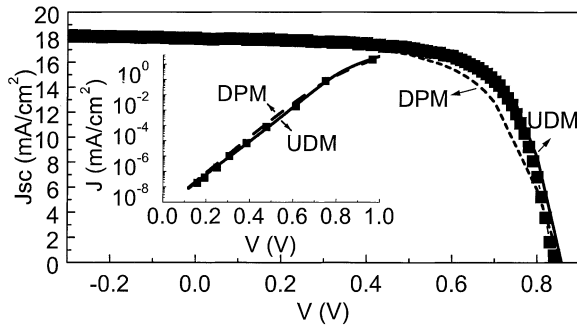


Fig. 1. Fitting of the illuminated current–voltage (J – V) characteristic of an a-Si:H p–i–n device adopting UDM in each layer and using the DPM. In the inset we show our fitting of the dark J – V curve. The intrinsic layer is 500 nm thick and the device is in the annealed state.

4. Impact of the decoupled state approximation in the output device characteristics of a-Si:H p–i–n solar cells

In this section we concentrate our discussion on the scenario where $U > 0$ and $\sigma_{\text{CH}} > \sigma_0$. This is the usual situation in a-Si:H-based devices.

In order to magnify the impact of using different DB representations in J – V and SR curves, we test in this paper an a-Si:H p–i–n device having a 1000 nm thick intrinsic layer with a uniform DB density of $5 \times 10^{16} \text{ cm}^{-3}$. Using the optical and electrical parameters extracted from our fittings, we intentionally adopt a higher density of DBs and a thicker intrinsic layer in order to weaken the electric field into the intrinsic layer and make our simulations more sensitive to the presence of DBs. In our fittings the correlation energy U is 0.2 eV and $\sigma_{\text{CH}} = 10 \times \sigma_0$.

When $U > 0$ and $\sigma_{\text{CH}} > \sigma_0$, the decoupled approach and the amphoteric approach predict practically the same low-forward and reverse dark J – V curve, with some minor differences in the high-forward dark J – V . In a-Si:H p–i–n devices the low-forward dark J – V is controlled by recombination and the high-forward J – V is controlled by electron SCLC over the virtual cathode [13]. The decoupled approach slightly decreases the high-forward current, meaning that the decoupled approach in the SCLC regime tends to overestimate electron trapping at the virtual cathode. However, as we

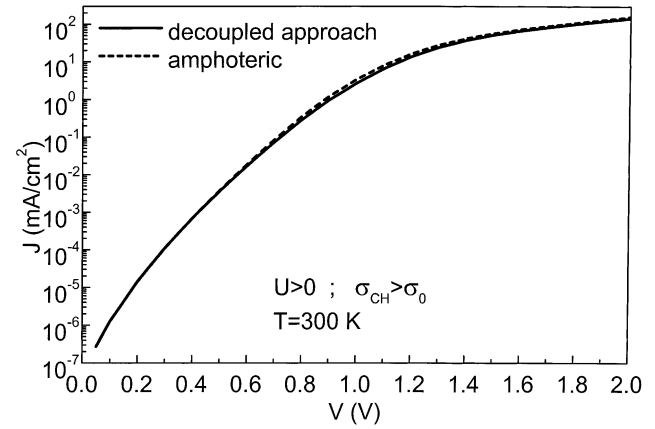


Fig. 2. Comparison of dark current–voltage characteristics evaluated with the decoupled approach and with the amphoteric approach in an a-Si:H p–i–n device where the intrinsic layer was assumed 1000 nm thick and the density of dangling bond adopted was $5 \times 10^{16} \text{ cm}^{-3}$. The correlation energy is 0.2 eV and capture cross-section for charged states is 10-fold higher than that for neutral states.

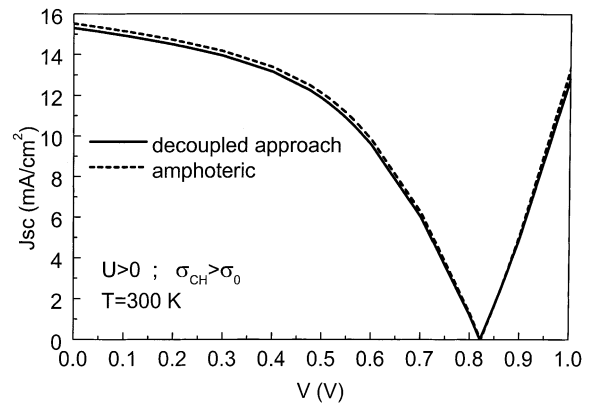


Fig. 3. Comparison of illuminated current–voltage characteristics evaluated with the decoupled approach and with the amphoteric approach in an a-Si:H p–i–n device where the intrinsic layer was assumed 1000 nm thick and the density of dangling bond adopted was $5 \times 10^{16} \text{ cm}^{-3}$. $U = 0.2 \text{ eV}$ and $\sigma_{\text{CH}} = 10 \times \sigma_0$.

can observe in Fig. 2, it is hard to note the difference at a single glance on a semi-log scale. Fig. 3 illustrates the illuminated J – V curve under AM1.5 light predicted by D-AMPS for the decoupled approach. The amphoteric approach gives rise to a higher short circuit current

Table 1

Total DB densities used in the UDM model and most probable dangling bond energy used in the DPM model for fitting purposes

	Layer					
	p-aSiC:H	ISiC1	ISiC2	ISiC3	i-a-Si:H	n-a-Si:H
UDM DB (cm^{-3})	2.64×10^{18}	1.25×10^{17}	6.25×10^{16}	2.50×10^{16}	5.00×10^{15}	6.78×10^{18}
UDM D^- (eV)	1.30	1.165	1.13	1.095	1.15	1.20
DPM E_p (eV)	1.30	1.22	1.20	1.18	1.17	1.17

There are three (i)a-SiC:H very thin layers with variable content of C between the p-a-SiC:H layer and the i-a-Si:H layer. They are recognized as ISiC1, ISiC2, and ISiC3.

(J_{sc}), implying that the decoupled approach tends to magnify recombination losses.

As discussed in Section 2, the decoupled approach could give rise to different trapped charge densities (which would alter the electrical field) and recombination rates. By looking at the trapped charge density profiles, we see small discrepancies in majority trapped carriers, but we see significantly higher minority trapped carrier densities predicted by the decoupled approach. This is agreement with the result found by Halpern. Fortunately, as the electric field is tailored by majority trapped carriers, significant errors in minority carrier concentrations do not significantly distort the electric field. At thermodynamic equilibrium and at low-forward and reverse voltages, D^- states and D^+ states clearly predominate in the vicinity of and inside of doped layers. On the other hand, when we focus an intense light on the front contact of a p-i-n device or when we apply a high-forward voltage, the whole device becomes more intrinsic.

Fig. 4a,b illustrate the relative errors introduced by the decoupled approach in the electron and hole trapped charged densities. These relative errors are defined as $\varepsilon_{NT} = 100 \times (n_{T2D} - n_{TAM}) / n_{TAM}$ and $\varepsilon_{PT} = 100 \times (p_{T2D} - p_{TAM}) / p_{TAM}$. In these equations, n_{T2D} (p_{T2D}) and n_{TAM} (p_{TAM}) are the trapped electron (hole) densities when the decoupled approach and the amphoteric approach are implemented. Similarly, we define the relative errors for the recombination rate as $\varepsilon_R = 100 \times (R_{2D} - R_{AM}) / R_{AM}$. The error ε_R is plotted in Fig. 4c. Our results in Fig. 4a seem to contradict the finding of Suntharalingam and Branz [8] and Willems [9]. These authors predicted errors only in the decoupled approach recombination rate, and no errors for the decoupled approach gap-state occupation functions for the conditions analyzed in this section. Our results indicate that, on the contrary, even in regions where one type of carrier clearly predominates, relative errors higher than 15% (over 10%, the ratio σ_0 / σ_{CH}) can be introduced in trapped carrier concentrations and in the recombination rate when DBs are approximated by donor and acceptor states. This apparent contradiction originates from the use of a self-consistent computer code. The above-mentioned authors compared the gap occupation function and the recombination rate separately in their analysis. In any computer code, an error introduced in the recombination rate affects the resultant free carrier concentrations and the gap-state occupation function values. Even if the two gap-state and exact occupation functions converge to an identical expression when $U > 0$ and $\sigma_{CH} > \sigma_0$, the error introduced in the recombination rate alters the trapped carrier concentrations through the differences introduced in the resulting free carrier concentrations. This is indeed observed in our simulations. Significant differences are observed in free carrier densities (not shown here) under illumina-

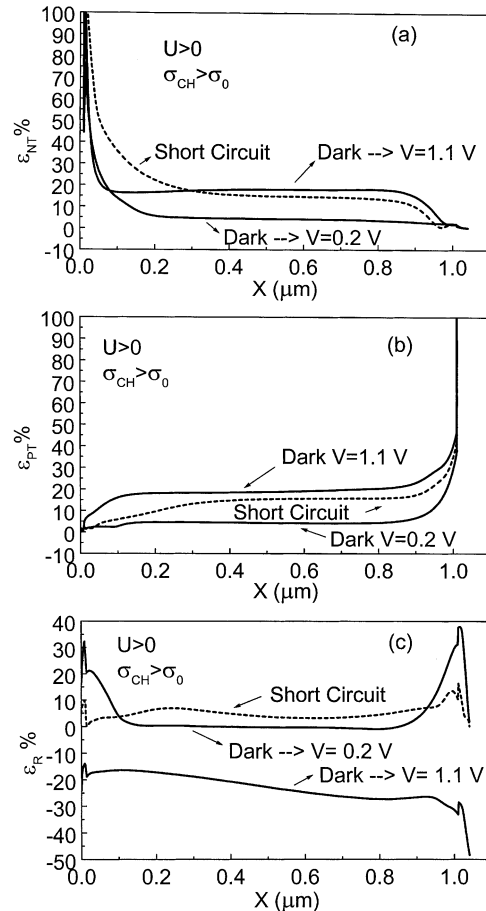


Fig. 4. Relative errors introduced by the decoupled approach in (a) trapped electron concentration, (b) trapped hole concentration and (c) recombination rate for the same device as in Figs. 2 and 3. These plots show the relative errors for two different voltages under dark conditions (0.2 and 1.1 V) and at short circuit conditions ($U > 0$, $\sigma_{CH} > \sigma_0$).

tion and under dark conditions at high forward bias, that not only change the trapped carrier densities in Gaussian functions (DB), but also the trapped carrier densities and recombination rates in tails where states are acceptor-like or donor-like. Fig. 4c indicates that the error in the recombination rate introduced by the decoupled approach could become more significant in regions where one carrier is clearly minority. The interdependence between free carrier densities and recombination rates gives rise to errors in the same recombination rate that are higher than the ratio between capture cross-section for neutral and charged states predicted by previous authors [8,9]. We can observe in Fig. 4c that these errors are highly position-dependent. Under dark conditions and reverse or low-forward voltage, the error in the recombination rate is higher near both doped layers. However, the decoupled approach is accurate in predicting the low-forward and the reverse dark $J-V$, because the most significant errors in the recombination

rates are located in regions where the recombination or generation rate is low. Under light and under high forward voltage and dark conditions, the material becomes more intrinsic and the recombination error spreads over the whole intrinsic layer. The decoupled approach seems to underestimate the recombination rate at high forward bias under dark conditions (see $V=1.1$ V). In reality, the decoupled approach overestimates the net electron and hole trapped concentrations (see Fig. 4a) on the virtual cathode and anode, which reduces the electron and hole currents injected into the intrinsic layer over the virtual cathode and anode, respectively. The lower availability of free carriers reduces the recombination present in the intrinsic layer. Looking at the relative errors introduced by the decoupled approach, we found for the p-i-n device of Figs. 2 and 3 a maximum value of 20% around the knee of the dark $J-V$. In the low-forward regimes, this error is below 5% and in the SCLC regime, below 10%. Hence, the dark $J-V$ could be modeled with the decoupled approach with some precaution. It works well at low-forward and reverse voltages, where concentrations of free carriers are small. When we increase the forward voltage, the feedback effect introduced by the decoupled approach into the trapped carrier concentrations through errors in the recombination rate and free carriers could lead to a non-negligible deviation from the exact dark $J-V$. This feedback effect is not present in single carrier devices where there is no recombination. Effectively, we found in n-type a-Si:H Schottky barriers extremely good agreement between the dark $J-V$ curves predicted by the decoupled approach and by the amphoteric approach. The relative error introduced by the decoupled approach is below 2%.

In order to quantify carefully the relative error introduced by the decoupled approach in solar cell modeling, we illustrate in Fig. 5 the maximum differences detected in the short circuit current (J_{sc}), fill factor (FF), open circuit voltage (V_{oc}), and efficiency (η) of a-Si:H-based p-i-n structures. The relative error introduced by the decoupled approach in the efficiency can be 2% (relative) in regular solar-cell structures and more than 3% in p-i-n structures with very thick and defective intrinsic layers. Similar results were obtained when the DPM was implemented in the p-i-n structure. The density of DBs predicted by the DPM varies between 2.0×10^{15} and $4.0 \times 10^{17} \text{ cm}^{-3}$ inside the intrinsic layer. These low errors indicate that the decoupled approach can be used in solar cell modeling. The decoupled approach works better under illumination than for high forward-voltage under dark conditions. Photo-generated free carriers do not have to be injected through virtual contact in which barrier heights are overestimated by the decoupled approach.

We tested the decoupled approach for device modeling at different temperatures in the range 200–450 K.

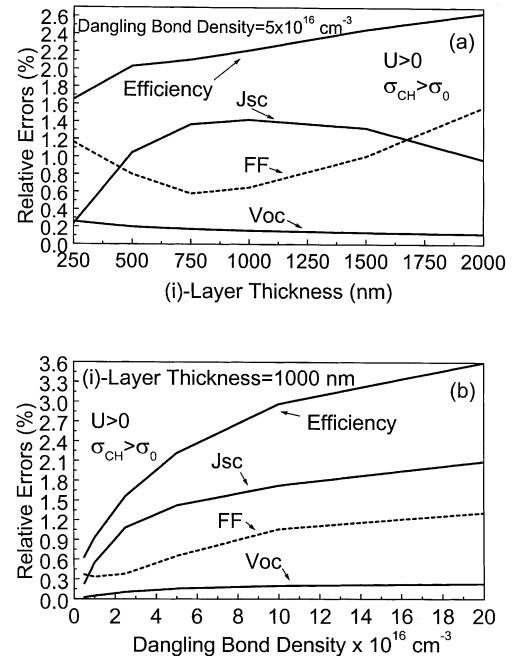


Fig. 5. (a) Relative error introduced by the decoupled approach in the short circuit current, open circuit voltage, fill factor and efficiency of an a-Si:H p-i-n with respect to the intrinsic layer thickness. The density of dangling bonds inside the i-layer is fixed to $5 \times 10^{16} \text{ cm}^{-3}$ ($U > 0$, $\sigma_{CH} > \sigma_0$). (b) Relative error introduced by the decoupled approach in the short circuit current, open circuit voltage, fill factor and efficiency of an a-Si:H p-i-n with respect to the density of dangling bonds. The intrinsic layer thickness is fixed to 1000 nm ($U > 0$, $\sigma_{CH} > \sigma_0$).

The maximum error introduced by the decoupled approach in the solar cell efficiency is practically temperature-independent within the range 300–350 K, and decreases at lower and higher temperatures. The error in estimating V_{oc} and J_{sc} decreases at lower and at higher temperatures, respectively. We also checked the decoupled approach for correlation energy U in the range 0.1–0.5 eV and found similar results.

5. The decoupled approach when the conditions $U \gg kT$ and $\sigma_{CH} > \sigma_0$ are not simultaneously fulfilled

5.1. $U > 0$ and capture cross-section $\sigma_{CH} < \sigma_0$

In this section we explore the accuracy of the decoupled approach when the correlation energy U is still positive but $\sigma_{CH} < \sigma_0$. Changing our capture cross-section, we can also check how sensitive this approximation is to the ratio between charged and neutral state capture cross-sections. We observe that when we decrease the ratio σ_{CH}/σ_0 , errors introduced by the decoupled approach are magnified.

Figs. 6 and 7 compare for the same p-i-n device studied above the dark and illuminated $J-V$ curves predicted by D-AMPS when the decoupled approach and

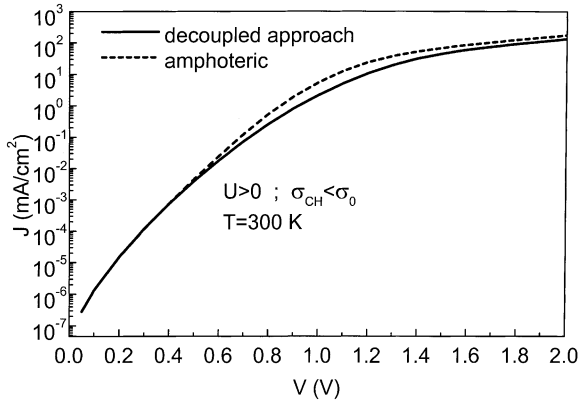


Fig. 6. Comparison of dark current–voltage characteristics evaluated with the decoupled approach and with the amphoteric approach in an a-Si:H p–i–n device where the intrinsic layer was assumed 1000 nm thick and the density of dangling bond adopted was $5 \times 10^{16} \text{ cm}^{-3}$. $U = 0.2 \text{ eV}$ and $\sigma_{\text{CH}} = 0.1 \times \sigma_0$.

the amphoteric approach are used. The correlation energy U is still equal to 0.2 eV, but the capture cross-section adopted are $\sigma_{\text{CH}} = \sigma_0/10$. Interestingly, in Fig. 6 we observe that the low-forward (and the reverse, not shown here) dark J – V is still well reproduced by the decoupled approach. Although at low-forward voltage in doped layers and near the p/i and i/n interfaces, we observe that $\varepsilon_{\text{R}} > 100\%$, surprisingly in the i-layer bulk where recombination peaks and defines the total current J , ε_{R} remains below 5%. At low-forward voltage the lower mobility of holes in a-Si:H situates the recombination rate peaks in the front part of the intrinsic layer near the crossover between the free electron concentration and the free hole concentration. In the scenario discussed in Section 4 and here, electrons control recombination at the left side of this crossover, where recombination is mainly through donor-like states, and holes control the recombination rate at the right side of this crossover, where recombination is mainly through acceptor-like states. When we change the ratio R_{C} , defined as $R_{\text{C}} = \sigma_{\text{CH}}/\sigma_0$, from 10 to 0.1 we interchange in the recombination kinetics the roles of the acceptor-like and donor-like Gaussian functions, but the overall recombination remains practically the same. Amphoteric states are not able to experience the difference. This result shows that in devices the error introduced in recombination by the decoupled approach does not necessarily follow the ratio R_{C} . At high-forward voltage in the i-layer bulk, ε_{R} is between 50 and 100% and ε_{NT} and ε_{PT} range between 30 and 60%. These errors are quite high and for the parameters used in our simulation lead to differences in the high-forward dark J – V characteristics of between 35 and 55%. In n-type Schottky barriers, the relative error in the dark J – V remains very low, which indicates that at high-forward voltage in p–i–n devices the recombination rate is responsible for the

errors introduced by the decoupled approach, by shaping the virtual cathode barrier shape. At high-forward voltage, recombination peaks near the p-layer. The connection between the recombination rate and the free carrier concentration indirectly affects the trapped charge densities to a major extent at high-forward voltage. Under illumination the error in evaluating J_{sc} increases to near 5%, but surprisingly the efficiency error is only 3.1%. In Fig. 7 we can clearly observe that differences between the two light J – V curves are considerable higher. However, for solar cell modeling, the relative errors at room temperature can be still tolerated. This is not the case at lower temperatures. For instance, at $T = 200 \text{ K}$ the relative error in the efficiency is near 30%.

5.2. The correlation energy U is negative

The correlation energy U is now negative and $\sigma_{\text{CH}} > \sigma_0$. This is the situation for selenium and chalcogenide glasses. For this scenario the decoupled approach is not able to satisfactorily describe the correct physics of dangling bonds. Figs. 8 and 9 show our results for the dark and light J – V characteristic curves of the same device studied in Section 3, but adopting a correlation energy U of -0.2 eV and $\sigma_{\text{CH}} = \sigma_0 \times 10$.

The current in the low-forward and reverse dark J – V is clearly higher in the decoupled approach that overestimates the recombination and generation rates. We find relative errors in the recombination (generation) rate at low-forward (reverse) voltage of over 400%. In the decoupled approach, although we do see important difference in trapped electron and trapped hole densities in Gaussian states that are confirmed by the Schottky barrier J – V , the net recombination rate is not significantly altered when the energy positions of acceptor-like and donor-like Gaussian peaks are exchanged. Recombination limited by electrons is still mainly through

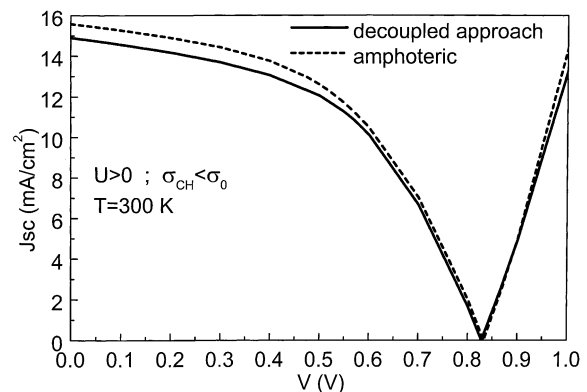


Fig. 7. Comparison of illuminated current–voltage characteristics evaluated with the decoupled approach and with the amphoteric approach in an a-Si:H p–i–n device where the intrinsic layer was assumed 1000 nm thick and the density of dangling bond adopted was $5 \times 10^{16} \text{ cm}^{-3}$. $U = 0.2 \text{ eV}$ and $\sigma_{\text{CH}} = 0.1 \times \sigma_0$.

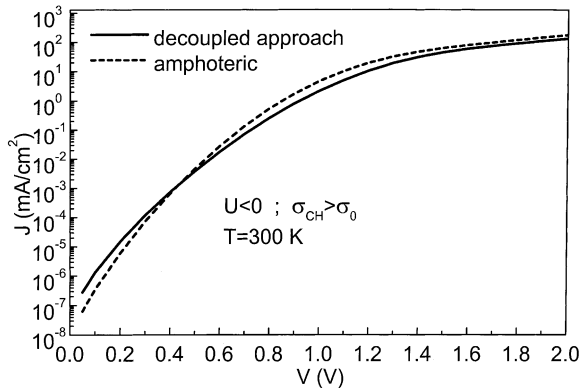


Fig. 8. Comparison of dark current–voltage characteristics evaluated with the decoupled approach and with the amphoteric approach in an a-Si:H p–i–n device where the intrinsic layer was assumed 1000 nm thick and the density of dangling bond adopted was $5 \times 10^{16} \text{ cm}^{-3}$. The correlation energy is -0.2 eV and $\sigma_{\text{CH}} = 10 \times \sigma_0$.

donor-like states, and recombination limited by holes is still mainly through acceptor-like states. On the other hand, in the amphoteric approach, recombination (generation) decreases significantly when we move from $U > 0$ to $U < 0$. Recombination processes at energy values below the mid-gap are not favored in the amphoteric approach when the U value adopted is negative. At high-forward bias, the current is lower in the decoupled approach, because in the SCLC regime this approach overestimates electron and hole trapping at the virtual cathode and anode, respectively, and the errors introduced in trapped charge density for this case are approximately 20%. In n-type Schottky barriers, errors of over 60% can be observed and, as in p–i–n devices, the high-forward dark J – V is underestimated by the decoupled approach. Finally, under illumination the error in J_{sc} is 2%, V_{oc} , 1%, FF, 6% and the efficiency, more

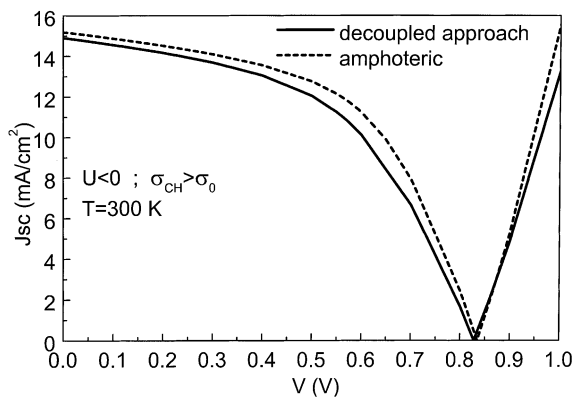


Fig. 9. Comparison of illuminated current–voltage characteristics evaluated with the decoupled approach and with the amphoteric approach in an a-Si:H p–i–n device where the intrinsic layer was assumed 1000 nm thick and the density of dangling bond adopted was $5 \times 10^{16} \text{ cm}^{-3}$. The correlation energy is -0.2 eV and $\sigma_{\text{CH}} = 10 \times \sigma_0$.

than 8%. The current in the light J – V curve and the spectral response are systematically predicted lower in the decoupled approach because this approximation magnifies the recombination rate. The same trends are observed no matter how the capture cross-section is adopted: $\sigma_{\text{CH}} > \sigma_0$, $\sigma_{\text{CH}} = \sigma_0$ or $\sigma_{\text{CH}} < \sigma_0$.

6. Conclusions

In a-Si:H-based devices, dangling bonds can be acceptably approximated as pairs of donor-like and acceptor-like states, as long as the correlation energy is assumed to be positive and the capture cross-sections of neutral states adopted are much smaller than those of charged states. The disadvantage of this simplification is a relative error not greater than 15 and 3% in the dark and illuminated current–voltage characteristics, respectively. Intrinsic layer thickness values in the range 500–2000 nm and density of states between 5×10^{15} and $2 \times 10^{17} \text{ cm}^{-3}$ have been investigated. The temperature was varied between 250 and 450 K. The decoupled approach leads us to unacceptable errors and fails in reproducing dark and illuminated J – V characteristic curves when the correlation energy adopted is negative. When $U > 0$ but $\sigma_0 > \sigma_{\text{CH}}$, we do not fully recommend the decoupled approach to model the high-forward dark J – V . In general, in device modeling we do not find a clear correlation between the relative errors introduced by the decoupled approach and the ratio between neutral and charged-state capture cross-sections.

Acknowledgments

We greatly appreciate the financial support of Agencia Nacional de Promoción Científica y Tecnológica, Project #10-00000-0095 and of the Netherlands Organization for Energy and Environment (NOVEM). We also thank Karine van der Werf for depositions and for the preparation of the solar cell samples.

References

- [1] R.A. Street, Hydrogenated Amorphous Silicon, Cambridge University Press, 1991.
- [2] H. Okamoto, H. Kida, Y. Hamakawa, Philos. Mag. B 49 (1984) 231.
- [3] R. Martins, A. Fantoni, M. Vieira, J. Non-Cryst. Solids 164–166 (1993) 671.
- [4] P. Chatterjee, J. Appl. Phys. 76 (2) (1994) 1301.
- [5] Technology Modeling Associates Inc, Medici, Two-Dimensional Device Simulation Program, Version 2.0, 1994.
- [6] V. Halpern, Philos. Mag. B 54 (1986) 473.

- [7] A. Rose, *Concepts in Photoconductivity and Allied Problems*, Robert E. Krieger, New York, 1978.
- [8] V. Suntharalingam, H.M. Branz, *Amorphous Silicon Technol.* 336 (1994) 153.
- [9] J.A. Willemen, *Modelling of Amorphous Silicon Single- and Multi-Junction Solar Cells*, PhD Thesis, Technische Universiteit Delft, 1998.
- [10] P.J. McElheny, J.K. Arch, H.S. Lin, S.J. Fonash, *J. Appl. Phys.* 64 (1988) 1254.
- [11] M.J. Powel, S.C. Deane, *Phys. Rev. B* 48 (1993) 10815.
- [12] M.J. Powel, S.C. Deane, *Phys. Rev. B* 53 (1996) 10121.
- [13] F.A. Rubinelli, H. Liu, C.R. Wronski, *Philos. Mag. B* 74 (1996) 407.